communications earth & environment

ARTICLE

https://doi.org/10.1038/s43247-022-00341-9 OPEN

Direct evidence for crust-mantle differentiation in the late Hadean

Alessandro Maltese [1,2]✉, Guillaume Caro[1], Om Prakash Pandey[3], Dewashish Upadhyay[4] & Klaus Mezger[2,5]

Constraints on the evolution of the silicate Earth between 4.5 and 3.8 billion years ago are limited by the scarcity of pristine geological material from that period. The geodynamic evolution of the early Earth, prior to the preserved rock record, is thus mainly inferred from numerical modelling. To evaluate the geological significance of these simulations, geochronological constraints pertaining to the evolution of the Hadean crust are required. Here we show using Neodymium isotope variations generated by decay of now-extinct 146-Samarium that Paleoarchean rocks from the Singhbhum Craton, India derived from a Hadean depleted mantle reservoir that differentiated $4.19^{+0.06}_{-0.12}$ billion years ago. The event postdates Neodymium model ages of mantle depletion inferred from other Archean rocks by 200 million years. This geochronological record is mirrored in the Hafnium isotope composition of the oldest zircon grains, suggesting that Hadean mantle differentiation proceeded via distinct pulses of large-scale magmatic activity and crustal rejuvenation.

[1] Université de Lorraine, CNRS, CRPG, 54000 Nancy, France. [2] Institute of Geological Sciences, University of Bern, Baltzerstrasse 1 + 3, 3012 Bern, Switzerland. [3] Department of Earth Sciences, Indian Institute of Technology Kanpur, 208016 Kanpur, India. [4] Department of Geology and Geophysics, Indian Institute of Technology Kharagpur, 721302 Kharagpur, India. [5] Center for Space and Habitability, University of Bern, Gesellschaftsstrasse 6, 3012 Bern, Switzerland. ✉email: alessandro.maltese@geo.unibe.ch

In the near-absence of a physically-preserved rock record prior to 4 Ga, insights into the extent and timing of earlier crust-mantle differentiation processes can either be obtained from scarce remnants of Hadean rocks (e.g. detrital zircons and their inclusions)[1–4] or using the geochemical and isotope composition of Archaean rocks. This chemical differentiation history ultimately reflects mantle dynamics and lithosphere tectonics during that time, which, due to a general lack of direct observations, is strongly reliant on numerical models[5,6]. To date, a wide range of tectonic modes have been defined that differ with respect to the cooling rate of a planet and the ability to cycle elements between its interior and exterior through volcanic and tectonic processes[7]. In active lid modes, such as modern-day plate tectonics, parts of the lithosphere sink back into the planet's interior, actively participating in mantle convection, and thus driving mantle cooling as well as continuous crustal growth and recycling[8,9]. The extent to which plate tectonics was operating in the early Earth remains widely debated, as higher mantle temperatures are thought to impede long-lived subduction and favour instead a stagnant-, sluggish-, or episodic-lid regime[7,10–13]. In the stagnant-lid mode, the lithosphere constitutes a single plate that does not take part in convective overturn, so that crustal rejuvenation occurs by other mechanisms such as heat-pipe volcanism and plume tectonics[14,15]. This mode predicts inefficient crustal recycling and shallow upper mantle convection, consistent with the long-term preservation of primordial mantle heterogeneities[16]. In a sluggish lid mode, the velocity of the mantle below the lithosphere exceeds surface velocities, resulting in slow plate motions and crustal recycling[13,17]. In the episodic-lid mode, stagnant phases alternate with short phases of extensive magmatic activity, leading to periodic mantle overturns and large-scale crustal rejuvenation[10,18,19].

Geodynamic models of the early Earth show varied outcomes for the longevity of the Hadean lithosphere, the occurrence and frequency of mantle overturns, and the timescales associated with convective re-homogenisation of differentiated mantle reservoirs[16,20]. Reconstruction of the differentiation history of the Hadean crust-mantle system can provide key temporal constraints on the tectonic evolution of the early Earth that would otherwise remain elusive due to the limited geological record. Short-lived radio-isotope systems, such as the ^{146}Sm–^{142}Nd chronometer, are particularly suited for this purpose. Due to its short half-life ($t_{1/2}$ = 103 Ma), the ^{146}Sm-^{142}Nd system selectively records crust-mantle differentiation events that took place >4 Gyr ago. Decay of ^{146}Sm in differentiated silicate reservoirs translates into heterogeneities in the abundance of its daughter isotope (^{142}Nd), which in turn can be transferred to the newly formed crust by re-melting of these ancient reservoirs. Using this approach, ^{142}Nd signatures reflecting the formation of both chemically enriched (crustal) and depleted (mantle) Hadean reservoirs have been identified in mantle-derived rocks from the oldest Archaean cratons[21–24]. Subsequent investigations of diverse Eo- to Neoarchean rocks[25–32] showed that the earliest stages of Earth's history were marked by extensive crust-mantle differentiation at 4.40 ± 0.03 Ga[32]. The apparent uniqueness of this event has been suggested to reflect a relatively quiescent evolution of the post-magma ocean Earth[16,26], or the extraction of large volumes of crust ca. 4.4–4.5 Gyr ago followed by rapid crustal recycling and rejuvenation through the Hadean[33]. Models advocating continuous crustal growth and recycling which require the ^{142}Nd composition of the depleted mantle to have gradually declined with time, are only weakly supported by the Archaean ^{142}Nd record[32]. However, the majority of ^{146}Sm–^{142}Nd studies have so far focused on Eoarchean rocks, and comparatively little is known about the evolution of the depleted mantle through the Archaean. Here we use combined ^{147,146}Sm–^{143,142}Nd systematics to show that the Paleoarchean mantle preserved large-scale heterogeneities related to a period of increased magmatic differentiation several hundred million years after crystallisation of the terrestrial magma ocean. Considered together with previous constraints, the Archaean ^{142}Nd record points towards at least two distinct episodes of Hadean crust-mantle differentiation. These events are also reflected in the Hf-isotope evolution of the oldest zircon grains. This concomitance of mantle depletion and crust extraction suggests that differentiation in the Hadean proceeded via distinct large-scale tectonomagmatic events that led to the creation of long-lived chemical heterogeneities in Earth's early mantle.

Results and discussion

For this study, igneous rocks from the Paleoarchean to Mesoarchean Bastar and Singhbhum cratons in India were investigated. Tonalite–trondhjemite–granodiorite (TTG) suites were sampled on a regional scale in the central to the western part of the Bastar Craton. Sample descriptions, locations, and zircon U-Pb ages ranging from about 3.45 to 3.55 Ga, are given in Maltese et al.[34]. Samples from the Singhbhum Craton were collected from the Older Metamorphic Tonalite Gneiss and all units of the Singhbhum Granite (Phase I to III). Sample locations, major and trace element compositions, and ^{147}Sm-^{143}Nd isotope data are published in Pandey et al.[35]. Zircon U-Pb ages are reported in Upadhyay et al.[36] and range from 3.47 to 3.29 Ga. Lutetium-Hf analyses on the same zircon grains by laser ablation inductively coupled plasma mass spectrometry yielded positive $\varepsilon^{176}Hf_i$ values up to +4, indicating the existence of a depleted mantle domain in the source region of the Singhbhum Craton granitoids[37]. In addition to the granitoids, samples of komatiitic, basaltic, and andesitic rocks from the Gorumahisani-Badampahar Iron Ore Group (IOG)[38], a supracrustal/greenstone belt near the eastern margin of the craton were also analysed. Investigated samples are those of Pandey et al.[35], who reported a whole-rock ^{147}Sm–^{143}Nd regression corresponding to 3.75 ± 0.34 Ga, in broad agreement with the emplacement age of 3510 ± 3 Ma inferred from U-Pb zircon dating[39].

Results of ^{146,147}Sm-^{142,143}Nd isotope analyses and age constraints are summarised in Supplementary Data 1 and displayed in Figs. 1 and 2. Following usual conventions, ^{142}Nd/^{144}Nd and initial ^{143}Nd/^{144}Nd are reported as relative deviations from the modern silicate Earth in parts per million (μ^{142}Nd) and from the chondritic uniform reservoir[40] in parts per ten thousand ($\varepsilon^{143}Nd_i$), respectively. The isotope composition of the Bastar granitoids range from −0.9 ± 2.8 ppm to 3.9 ± 3.2 ppm for μ^{142}Nd and from −1.3 to +1.3 for $\varepsilon^{143}Nd_i$, but have an average composition close to that of the primitive mantle (Supplementary Data 1). In contrast, the isotope composition of the Singhbhum granitoids displays a spread in μ^{142}Nd values ranging from −2.0 ± 3.6 ppm to +6.3 ± 4.6 ppm which are positively correlated with $\varepsilon^{143}Nd_i$ ($\varepsilon^{143}Nd_i$ = −0.5 to +5.1). No clear relationship is observed between the ^{142,143}Nd composition of the granitoids and their U-Pb ages or bulk-rock chemistry. Specifically, five samples with μ^{142}Nd values indistinguishable from bulk silicate Earth also have $\varepsilon^{143}Nd_i$ within ±1 ε-unit of the chondritic value, while four samples that exhibit a resolved positive μ^{142}Nd anomaly (i.e., +3.9 to +6.3) have positive $\varepsilon^{143}Nd_i$ values (i.e., +2.5 to + 5.1). Similarly-radiogenic initial Nd isotope compositions are obtained for the mafic and ultramafic rocks from the 3.51 Ga eastern IOG, with μ^{142}Nd between +1.2 and +6.3, and $\varepsilon^{143}Nd_i$ between +0.9 and +3.8 (Supplementary Data 1). The ^{146}Sm–^{142}Nd and ^{147}Sm–^{143}Nd data, therefore, provide concordant results for all investigated units of the Singhbhum and Bastar cratons—the granitoids of the Bastar Craton bear no record of early differentiation, whereas part of the Singhbhum granitoids and associated supracrustal rocks of the IOG formed from isotopically

heterogeneous material originally derived from mantle domains depleted in the Hadean (Fig. 2).

Evidence for late Hadean differentiation. The differentiation history of the Paleoarchean Singhbhum TTGs and supracrustal rocks from the IOG can be further constrained by coupled ^{146,147}Sm–^{142,143}Nd chronometry, assuming a two-stage model as a first-order approximation of the evolution of their mantle source[22,32]. The first stage corresponds to the evolution of a chondritic reservoir from ~4.57 Ga (T_0) to an instantaneous differentiation event at T_D that produced a depleted mantle reservoir (DM). The second stage describes the closed-system evolution of this source reservoir from T_D until formation of the Singhbhum Craton at T_S as a function of its Sm/Nd ratio (^{147}Sm/^{144}Nd$_{src}$). By combining the two chronometric equations of the ^{146,147}Sm–^{142,143}Nd system, both the time of differentiation of the depleted mantle as well as its time-integrated ^{147}Sm/^{144}Nd$_{src}$ can be estimated (see 'Methods' section, Supplementary Fig. S-2). This allows eliminating uncertainties of conventional model ages related to the composition of the parent Hadean mantle reservoir. The two-stage model indicates differentiation of the Singhbhum TTG source reservoir at $4.19^{+0.06}_{-0.12}$ Ga, with ^{147}Sm/^{144}Nd$_{src}$ ranging from near-chondritic to 0.25 (Fig. 1). Samples from the IOG belt yield a similar model age and time-integrated ^{147}Sm/^{144}Nd$_{src}$, albeit with larger uncertainties, likely caused by imperfect preservation of their ^{147}Sm–^{143}Nd systematics or improper age assignment (see Supplementary Discussion). Despite these limitations, the model age estimated for the IOG supracrustal rocks is broadly similar to that inferred from the Singhbhum granitoids (Fig. 1 and Supplementary Fig. S-1). These chronological constraints are distinct from those obtained by coupled ^{146,147}Sm–^{142,143}Nd systematics from Eoarchean terranes of southwest Greenland and northern Labrador which yielded an older model age of 4.40 ± 0.03 Ga together with a lower time-integrated ^{147}Sm/^{144}Nd$_{src}$ of 0.21[32]. Although more complex evolution scenarios cannot be excluded, the concordant ^{142,143}Nd model ages obtained from various Archaean cratons suggest that despite these simplified assumptions, a two-stage differentiation history constitutes a generally valid framework that can approximate the evolution of Hadean silicate reservoirs. The simplest interpretation, therefore, is that the isotope signatures of the Singhbhum rocks reflect a late Hadean mantle depletion event while the Bastar Craton formed from more primitive mantle domains that bear no record of Hadean differentiation (Fig. 2). Collectively, these results demonstrate that the Archaean mantle comprised both large-scale primitive and chemically depleted

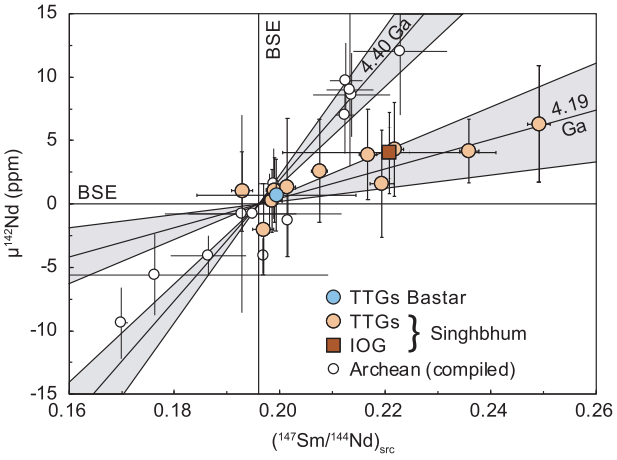

Fig. 1 Model ages of mantle depletion. Isochron diagram showing the ^{142}Nd isotope composition of Bastar and Singhbhum samples against the (^{147}Sm/^{144}Nd)$_{src}$ ratio of their respective mantle sources. (^{147}Sm/^{144}Nd)$_{src}$ is obtained from two-stage isotope evolution modelling of coupled ^{146,147}Sm-^{142,143}Nd systematics (Supplementary Methods). Additional data from Archaean cratons (open circles) mark the onset of global crust-mantle differentiation at 4.4 ± 0.03 Ga (references in the text). Grey-shaded envelopes mark model age uncertainties. Error bars are 2 SE for single analyses and 2 SD for replicated analyses (Supplementary Data 1). Reference lines for bulk silicate Earth (BSE) are shown for context.

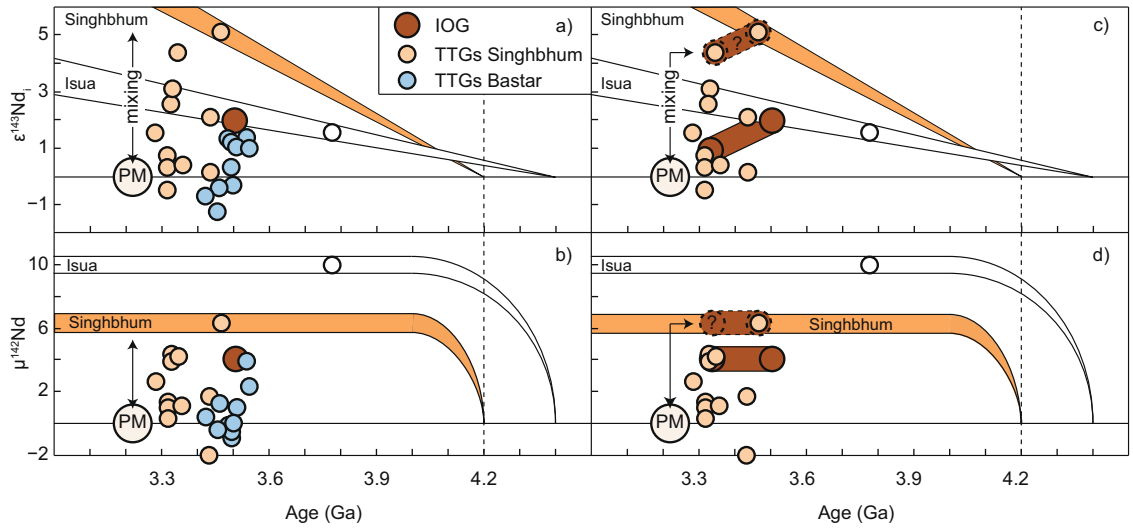

Fig. 2 ^{147}Sm–^{143}Nd and ^{146}Sm–^{142}Nd isotope evolution of the Singhbhum mantle source and petrogenesis. The tiles illustrate two possible petrogenetic scenarios for the formation of mafic rocks from the IOG greenstone belt and TTGs from the Singhbhum Craton. Panels **a** and **b** consider only the isotope composition of the source melts such that the vertical spread defined by TTGs in Nd isotope vs. time space reflects mixing of melts derived from both depleted and primitive mantle (PM) domains. Panels **c** and **d** also consider the petrogenesis of TTGs which were likely produced by re-melting of a mafic protolith, here represented by the 3.51 Ga supracrustal rocks from the eastern IOG belt. In this scenario, the most radiogenic Nd isotope compositions require a so-far elusive mafic precursor extracted from the depleted mantle shortly before formation of the granitoids. The distinct evolution of the Isua depleted mantle reservoir is shown for comparison.

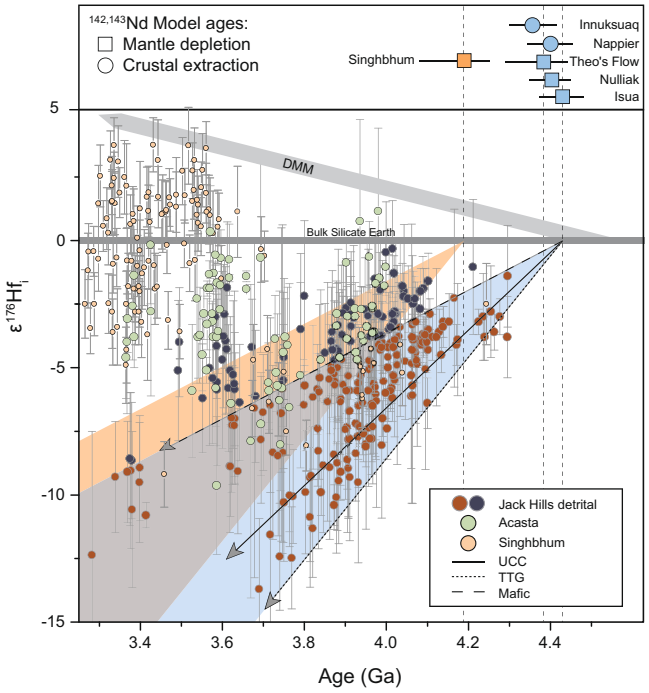

Fig. 3 Comparison of Nd and Hf model ages of mantle depletion and crustal extraction. a Summary of published model ages of crust-mantle differentiation inferred from coupled ^{146,147}Sm-^{142,143}Nd chronometry[32,56]. **b** Compilation of zircon Hf-isotope compositions and associated 2 SD external reproducibility; detrital zircon data from the Jack Hills metaconglomerate[3,4] (dark red/blue), igneous zircon from the Acasta Gneiss Complex[43,45] (green), and detrital and xenocrystic zircon from the Singhbhum Craton[41,42] (orange). The DMM (depleted MORB mantle) approximates the isotope evolution of Earth's upper mantle from its origin ($\varepsilon^{176}Hf_i = 0$ at 4.4–4.5 Ga) to the present-day ($\varepsilon^{176}Hf_i \approx +15$). The coloured arrays (blue and orange) show the expected isotope evolution of juvenile crust extracted from a primitive mantle reservoir (bulk silicate Earth) at 4.42 Ga and 4.19 Ga. The arrays are bound by the isotope trajectories of a mafic reservoir with $^{176}Lu/^{177}Hf$ of 0.022, a tonalite–trondhjemite–granodiorite (TTG) reservoir with $^{176}Lu/^{177}Hf$ of 0.005; a crustal reservoir with $^{176}Lu/^{177}Hf$ of 0.008, corresponding to the average upper continental crust (UCC), is shown for comparison[3,4]. Dark red data points show zircon grains with initial $\varepsilon^{176}Hf$ consistent with differentiation of their protoliths during an early crust formation event at ~4.4 Ga. Dark blue circles represent zircon grains with initial $\varepsilon^{176}Hf$ requiring a younger crustal protolith, consistent with zircon data on Acasta and Singhbhum.

domains. Some of these depleted domains were produced during or shortly after the end of terrestrial accretion, possibly as a result of magma ocean crystallisation, while others, like the Singhbhum source region, may reflect crust extraction in the late Hadean.

A coeval record of crustal extraction and mantle depletion. Geochemical evidence for Hadean crust formation can be found in the Hf-isotope record of Hadean and Eoarchean zircon[1–4,41]. Previous studies showed that the majority of Hadean/Eoarchean zircon grains define an array in $\varepsilon^{176}Hf_i$ vs. time space (with values becoming more negative with decreasing age) which is interpreted to reflect reworking of Earth's primordial crust that differentiated 4.4–4.5 Gyr ago[3,4,41] (Fig. 3). This event is also recorded in rare zircon xenocrysts in Paleoarchean TTGs and detrital zircon from younger siliciclastic successions from the Singhbhum Craton[41,42]. As shown in Fig. 3, this event is well reflected in the crust-mantle differentiation ages of ~4.4 Ga inferred from the ^{146,147}Sm–^{142,143}Nd systematics of Eoarchean rocks. In addition, several studies pointed out the presence of a population of Hadean grains, at 3.9–4.1 Ga, with $\varepsilon^{176}Hf_i$ above plausible evolution lines for a 4.4–4.5 Gyr old crustal reservoir[3,4] (Fig. 3). This bulge in the $\varepsilon^{176}Hf_i$ vs. time array requires differentiation of crustal protoliths from juvenile magmas produced in the late Hadean and subsequent evolution of this crustal domain with a time-integrated $^{176}Lu/^{177}Hf$ ratio between that of mafic and felsic rocks (Fig. 3). A similar late Hadean (~4.2 Ga) crustal extraction age was also inferred for the precursor of the ca. 3.9–4.0 Ga Acasta gneisses[43–46] (Fig. 3), in agreement with the identification of a 4.203 ± 0.058 Ga zircon xenocryst in a granitic rock of the complex[47]. As is the case for the differentiation event at ~4.4 Ga, crust generation at ~4.2 Ga is also reflected both in the extinct nuclide record of mantle depletion and in the surviving relics of the Hadean rock record. This observation seemingly conflicts with the notion that Hadean crustal extraction ages reflect sporadic preservation of small crustal domains[33], as this would not necessarily involve the preservation of their complementary depleted reservoir in the convective mantle. Rather, the record of coeval crust extraction and mantle depletion points to the occurrence of at least two major crust forming events in the Hadean. These events produced depleted mantle domains large enough to escape complete re-homogenisation on a billion-year timescale.

A temporal frame for geodynamic models. Geodynamic simulations suggest that Hadean-Archaean tectonics may have been dominated by vertical exchanges between the mantle and crust[18,48,49]. Consistent with this interpretation are studies on Archaean supracrustal belts which show that terranes with geochemical characteristics indicative of subduction settings were uncommon and rather dominated by volcanic rocks, reflecting embryonic stages of arc formation[50,51]. In the possible absence of self-sustained subduction, crust generation and recycling in the early Earth may have proceeded sporadically[11,12,49], in response to disruptive events such as large plumes[15] and impacts[12], or due to dripping of gravitationally unstable parts of the lithosphere[10,18]. Consistent with our observations, such catastrophic events would produce large depleted mantle domains during short pulses (~10–20 Myr) of extreme magmatic activity interspersed by long periods of relative quiescence[10,18,19]. Models advocating an episodic-lid behaviour further impart a strong periodicity in the tectonic evolution of the early Earth[19], which may be reflected in the ~200 Myr time period separating the two major mantle depletion events recorded by the ^{146}Sm–^{142}Nd system. In light of the currently available data, it thus appears unlikely that an active tectonic regime, akin of plate tectonics, was operating on the Hadean Earth. Going beyond these different scenarios, our results provide the first evidence that Hadean crust generation is consistently reflected both in the history of mantle depletion and in the geological relics of that epoch. Further investigations of these fragmentary records thus have the potential to assess the frequency of crust-mantle differentiation events during the Hadean as well as the composition of these differentiated reservoirs. Ultimately, chronological constraints on Hadean crust-mantle differentiation, as obtained from the ^{146,147}Sm–^{142,143}Nd isotope systems, may complement geophysical approaches and help to evaluate and refine models of ancient Earth's geodynamics.

Methods

Data acquisition. Whole-rock powders were obtained using standard rock crushing techniques. Details for combined ^{147}Sm-^{143}Nd isotope dilution and $^{143}Nd/^{144}Nd$ isotope composition determination, conducted at the University of Bern, are described in Pandey et al.[35] with the corresponding data displayed in Supplementary Data 1. Data on the Bastar Craton were obtained during this study following the same protocols, but using inductively coupled plasma mass spectrometry. An average $^{143}Nd/^{144}Nd$ ratio of 0.512078 ± 5 (2 SD, $n = 14$) was obtained for repeated measurements of the JNdi-1 standard solution during the course of the study (Supplementary Data 2). The external reproducibility of $^{143}Nd/$

^{144}Nd for samples was estimated using the relationship between the external reproducibility of JNdi-1 measurements over the course of the study (% 2 SD, $n = 14$) and the average standard error of individual analyses (% 1 SE, 60 × 8 s integrations). All samples were normalised to the recommended JNdi-1 ^{143}Nd/^{144}Nd value of 0.512115 for international comparison[52]. Element purification and isotope analyses for ^{146}Sm–^{142}Nd investigation of all samples were performed at CRPG, Nancy using protocols detailed in Morino et al.[32]. Neodymium isotope measurements were performed by thermal ionisation mass spectrometry, using a two-line multidynamic scheme. Correction for mass fractionation drift during acquisition[53] was performed following Morino et al.[32]. Measurements were performed in three analytical sessions during which the external precision, expressed as 2 SD, was estimated by repeated measurement of the JNdi-1 standard at 3.2 ppm, 1.3 ppm, and 2.6 ppm, respectively (Supplementary Data 2). ^{143}Nd/^{144}Nd ratios are reported using the conventional ε-notation, as relative deviation in parts per 10,000 from the chondritic value[40]. ^{142}Nd/^{144}Nd ratios are reported in μ-notation, as deviation in ppm from the JNdi-1 reference material. Internal run statistics (2 standard error, SE) are reported for samples that were analysed once. Replicate analyses are reported using the average value and an uncertainty of 2.5 ppm corresponding to the average 2 SD reproducibility of standards from all analytical sessions. For model calculations, an initial ^{146}Sm/^{144}Sm of 0.0082 was used in conjunction with a half-life of 103 Myr for ^{146}Sm[54,55].

Coupled ^{146,147}Sm-^{142,143}Nd model age calculations. The chronological implications of the investigated rock suites are examined using a two-stage isotope evolution model. The first stage corresponds to the evolution of a primitive reservoir (bulk silicate Earth, BSE) between the origin of the solar system ($T_0 = 4.567$ Ga) and an instantaneous differentiation event at $T = T_D$. The second stage represents the closed-system evolution of differentiated silicate reservoirs between T_D and the crystallisation age of the samples at $T = T_S$. The ^{142,143}Nd/^{144}Nd composition of the depleted mantle source reservoir (src) at T_S is given by:

$$\left(\frac{^{143}\mathrm{Nd}}{^{144}\mathrm{Nd}}\right)_{\mathrm{src}}^{T_S} = \left(\frac{^{143}\mathrm{Nd}}{^{144}\mathrm{Nd}}\right)_{\mathrm{BSE}}^{T_P} + \left(\frac{^{147}\mathrm{Sm}}{^{144}\mathrm{Nd}}\right)_{\mathrm{BSE}}^{T_P} \times \left(1 - e^{\lambda_{147} T_D}\right) + \left(\frac{^{147}\mathrm{Sm}}{^{144}\mathrm{Nd}}\right)_{\mathrm{src}}^{T_P} \times \left(e^{\lambda_{147} T_D} - e^{\lambda_{147} T_S}\right) \quad (1)$$

$$\left(\frac{^{142}\mathrm{Nd}}{^{144}\mathrm{Nd}}\right)_{\mathrm{src}}^{T_S} = \left(\frac{^{142}\mathrm{Nd}}{^{144}\mathrm{Nd}}\right)_{\mathrm{BSE}}^{T_P} + \frac{(^{146}\mathrm{Sm}/^{144}\mathrm{Sm})_{T_0}}{(^{147}\mathrm{Sm}/^{144}\mathrm{Sm})_{T_P}} \times \left[\left(\frac{^{147}\mathrm{Sm}}{^{144}\mathrm{Nd}}\right)_{\mathrm{BSE}}^{T_P} \times \left(e^{-\lambda_{146} T_0} - e^{-\lambda_{146}(T_0 - T_D)}\right) + \left(\frac{^{147}\mathrm{Sm}}{^{144}\mathrm{Nd}}\right)_{\mathrm{src}}^{T_P} \times \left(e^{-\lambda_{146}(T_0 - T_D)} - e^{-\lambda_{146}(T_0 - T_S)}\right)\right] \quad (2)$$

where $\lambda_{146} = 6.74 \times 10^{-9}$ a^{-1} and $\lambda_{147} = 6.54 \times 10^{-12}$ a^{-1} are the decay constants for ^{146}Sm and ^{147}Sm, respectively, and T_P refers to the present-day. The ^{147}Sm/^{144}Nd and ^{143}Nd/^{144}Nd ratios of the bulk silicate Earth are considered chondritic[39]. The ^{142}Nd/^{144}Nd composition of the BSE is estimated by repeated measurements of the JNdi-1 international standard.

For each sample carrying a positive ^{142}Nd anomaly, the corresponding (^{147}Sm/^{144}Nd)$_{src}$ and T_D can be calculated by solving Eqs. (1) and (2) iteratively. The first iteration assumes an arbitrary value of $T_D = 4.5$ Ga and the corresponding (^{147}Sm/^{144}Nd)$_{src}$ is then calculated using Eq. (1). This value is then inserted into Eq. (2) to derive a new value of T_D. This calculation is repeated until constant values of T_D and (^{147}Sm/^{144}Nd)$_{src}$ are obtained. Alternatively, a two-stage model age can be calculated by combining all samples within a ^{146,147}Sm-^{142,143}Nd isochron (Supplementary Fig. S-2). This approach is similar to that presented above but presents the advantage of integrating all the isotope information into the age calculation. In this case, it is assumed that all samples are derived from cogenetic (mantle) domains with different parent-daughter ratios, or alternatively, that the chemical and isotopic heterogeneities that define the slope of the μ^{142}Nd–Sm/Nd array result from mixing between a Hadean depleted reservoir and a primitive mantle component. The model age is calculated by regression of the ^{142}Nd/^{144}Nd vs. (^{144}Sm/^{144}Nd)$_{src}$ array (Supplementary Fig. S-2). For samples showing no significant ^{142,143}Nd excess, (^{147}Sm/^{144}Nd)$_{src}$ is approximated using Eq. (2), assuming a value of $T_D = 4.2$ Ga. As those samples are characterised by $\varepsilon^{143}Nd_i \approx 0$, the calculation yields near-chondritic (^{147}Sm/^{144}Nd)$_{src}$ and this result is thus only marginally dependent on the assumed value of T_D. The slope of the regression line (Fig. S-2) is equal to the value of the ^{146}Sm/^{144}Sm ratio at T_D, and the differentiation age is then obtained using the decay equation:

$$T_D = -(1/\lambda_{146}) \times \ln\left[\frac{(^{146}\mathrm{Sm}/^{144}\mathrm{Sm})_{T_d}}{(^{146}\mathrm{Sm}/^{144}\mathrm{Sm})_{T_0}}\right] \quad (3)$$

where $(^{146}\mathrm{Sm}/^{144}\mathrm{Sm})_{T_0} = 0.0082$ is the initial isotope composition of the solar system and $\lambda_{146} = 6.73\ 10^{-3}$ Ma^{-1} is the decay constant of ^{146}Sm[54,55].

The Singhbhum results, represented in Fig. S-1, show that the four granitoid samples with the most positive $\varepsilon^{143}Nd_i$ values (i.e., +2.5 to +5.1) and positive μ^{142}Nd values (+3.9 to +6.3 ppm) yield similar two-stage model ages ranging from 4.18 Ga to 4.26 Ga (Supplementary Fig. S-1a), with an average $T_D = 4.22 \pm 0.07$ Ga (2 SD) similar to the model age derived from the ^{146,147}Sm–^{142,143}Nd isochron ($4.19^{+0.06}_{-0.12}$ Ga, Fig. 1). Despite the possibility of minor open system behaviour in the investigated IOG rocks, a model age can tentatively be estimated by back-calculating the initial ε^{143}Nd compositions to the accepted emplacement age of 3.51 Ga[39], or alternatively by using the $\varepsilon^{143}Nd_i$ of 2.4 ± 1 obtained from the 3.75 Ga isochron regression (see Supplementary Discussion, Pandey et al.[35]). Considered together with the average μ^{142}Nd of 4.1 ± 3.2 ppm, these calculations yield imprecise but broadly similar late Hadean model ages of 4.27 ± 0.22 Ga and 4.15^{+11}_{-20} Ga, respectively (Supplementary Fig. S-1b, c).

Data availability

All isotope geochemical data related to this article are available in the online Supplementary Material (Supplementary Data 1 and 2). In addition, all data have been uploaded to the EarthChem Library, available under https://doi.org/10.26022/IEDA/112197.

Received: 29 September 2021; Accepted: 21 December 2021;
Published online: 18 January 2022

References

1. Harrison, T. M. et al. Heterogeneous Hadean hafnium: evidence of continental crust at 4.4 to 4.5 Ga. *Science* **310**, 1947–1950 (2005).
2. Harrison, T. M., Schmitt, A. K., McCulloch, M. T. & Lovera, O. M. Early (≥4.5 Ga) formation of terrestrial crust: Lu-Hf, δ18O, and Ti thermometry results for Hadean zircons. *Earth Planet. Sci. Lett.* **268**, 476–486 (2008).
3. Kemp, A. I. S. et al. Hadean crustal evolution revisited: New constraints from Pb-Hf isotope systematics of the Jack Hills zircons. *Earth Planet. Sci. Lett.* **296**, 45–56 (2010).
4. Bell, E. A., Harrison, T. M., Kohl, I. E. & Young, E. D. Eoarchean crustal evolution of the Jack Hills zircon source and loss of Hadean crust. *Geochim. Cosmochim. Acta* **146**, 27–42 (2014).
5. Gerya, T. Precambrian geodynamics: concepts and models. *Gondwana Res.* **25**, 442–463 (2014).
6. Sobolev, S. V. & Brown, M. Surface erosion events controlled the evolution of plate tectonics on Earth. *Nature* **570**, 52–57 (2019).
7. Lenardic, A. The diversity of tectonic modes and thoughts about transitions between them. *Philos. Trans. R. Soc.* A **376**, 20170416 (2018).
8. Schubert, G., Turcotte, D. L. & Olson, P. *Mantle Convection in the Earth and Planets* (Cambridge Univ. Press, Cambridge, 2001).
9. Bercovici, D., Tackley, P. & Ricard, Y. In *Treatise Geophys* (ed. Schubert, G.) 271–318 (2015).
10. van Thienen, P., van den Berg, A. P. & Vlaar, N. J. Production and recycling of oceanic crust in the early Earth. *Tectonophysics* **386**, 41–65 (2004).
11. Fischer, R. & Gerya, T. Regimes of subduction and lithospheric dynamics in the Precambrian: 3D thermomechanical modelling. *Gondwana Res.* **37**, 53–70 (2016).
12. O'Neill, C., Marchi, S., Zhang, S. & Bottke, W. Impact-driven subduction on the Hadean Earth. *Nat. Geosci.* **10**, 793–797 (2017).
13. Foley, B. J. The dependence of planetary tectonics on mantle thermal state: applications to early Earth evolution. *Philos. Trans. R. Soc. A* **376**, 20170409 (2018).
14. Moore, W. B. & Webb, A. A. G. Heat-pipe earth. *Nature* **501**, 501–505 (2013).
15. Gerya, T. V., Stern, R. J., Baes, M., Sobolev, S. V. & Whattam, S. A. Plate tectonics on the Earth triggered by plume-induced subduction initiation. *Nature* **527**, 221–225 (2015).
16. Debaille, V. et al. Stagnant-lid tectonics in early Earth revealed by 142Nd variations in late Archean rocks. *Earth Planet. Sci. Lett.* **373**, 83–92 (2013).
17. Solomatov, V. S. Scaling of temperature- and stress-dependent viscosity convection. *Phys. Fluids* **7**, 266–274 (1995).
18. Fischer, R. & Gerya, T. Early Earth plume-lid tectonics: a high-resolution 3D numerical modelling approach. *J. Geodyn.* **100**, 198–214 (2016).
19. Stamenković, V., Höink, T. & Lenardic, A. The importance of temporal stress variation and dynamic disequilibrium for the initiation of plate tectonics. *J. Geophys. Res. E Planets* **121**, 896–915 (2016).
20. Foley, B. J. & Rizo, H. Long-term preservation of early formed mantle heterogeneity by mobile lid convection: Importance of grainsize evolution. *Earth Planet. Sci. Lett.* **475**, 94–105 (2017).
21. Harper, C. L. & Jacobsen, S. B. Evidence from coupled 147Sm-143Nd and 146Sm-142Nd systematics for very early (4.5-Gyr) differentiation of the Earth's mantle. *Nature* **360**, 728–732 (1992).
22. Caro, G., Bourdon, B., Birck, J. L. & Moorbath, S. 146Sm-142Nd evidence from Isua metamorphosed sediments for early differentiation of the Earth's mantle. *Nature* **423**, 428–432 (2003).

23. Boyet, M. et al. 142Nd evidence for early Earth differentiation. *Earth Planet. Sci. Lett.* **214**, 427–442 (2003).
24. O'Neil, J., Carlson, R. W., Francis, D. & Stevenson, R. K. Neodymium-142 evidence for Hadean mafic crust. *Science.* **321**, 1828–1831 (2008).
25. Caro, G., Bourdon, B., Wood, B. J. & Corgne, A. Trace-element fractionation in Hadean mantle generated by melt segregation from a magma ocean. *Nature* **436**, 246–249 (2005).
26. Caro, G., Morino, P., Mojzsis, S. J., Cates, N. L. & Bleeker, W. Sluggish Hadean geodynamics: Evidence from coupled 146,147Sm–142,143Nd systematics in Eoarchean supracrustal rocks of the Inukjuak domain (Québec). *Earth Planet. Sci. Lett.* **457**, 23–37 (2017).
27. Bennett, V. C., Brandon, A. D. & Nutman, A. P. Coupled 142Nd-143Nd isotopic evidence for Hadean mantle dynamics. *Science* **318**, 1907–1910 (2007).
28. Rizo, H., Boyet, M., Blichert-Toft, J. & Rosing, M. T. Early mantle dynamics inferred from 142Nd variations in Archean rocks from southwest Greenland. *Earth Planet. Sci. Lett.* **377–378**, 324–335 (2013).
29. Roth, A. S. G. et al. Inherited 142Nd anomalies in Eoarchean protoliths. *Earth Planet. Sci. Lett.* **361**, 50–57 (2013).
30. Roth, A. S. G. et al. Combined 147,146Sm-143,142Nd constraints on the longevity and residence time of early terrestrial crust. *Geochem. Geophys. Geosyst.* **15**, 2329–2345 (2014).
31. Puchtel, I. S., Blichert-Toft, J., Touboul, M., Horan, M. F. & Walker, R. J. The coupled 182W-142Nd record of early terrestrial mantle differentiation. *Geochem. Geophys. Geosyst.* **17**, 2168–2193 (2016).
32. Morino, P., Caro, G., Reisberg, L. & Schumacher, A. Chemical stratification in the post-magma ocean Earth inferred from coupled 146,147Sm–142,143Nd systematics in ultramafic rocks of the Saglek block (3.25–3.9 Ga; northern Labrador, Canada). *Earth Planet. Sci. Lett.* **463**, 136–150 (2017).
33. Rosas, J. C. & Korenaga, J. Rapid crustal growth and efficient crustal recycling in the early Earth: Implications for Hadean and Archean geodynamics. *Earth Planet. Sci. Lett.* **494**, 42–49 (2018).
34. Maltese, A., Mezger, K., Berndt, J., Upadhyay, D. & Scherer, E. E. On the petrogenesis of Paleoarchean continental crust: U-Pb-Hf isotope and major-trace element constraints from the Bastar Craton, India. *Chem. Geol.* **579**, 120337 (2021).
35. Pandey, O. P. et al. Genesis of the Singhbhum Craton, eastern India; implications for Archean crust-mantle evolution of the Earth. *Chem. Geol.* **512**, 85–106 (2019).
36. Upadhyay, D., Chattopadhyay, S., Kooijman, E., Mezger, K. & Berndt, J. Magmatic and metamorphic history of Paleoarchean tonalite-trondhjemite-granodiorite (TTG) suite from the Singhbhum craton, eastern India. *Precambrian Res.* **252**, 180 (2014).
37. Upadhyay, D., Chattopadhyay, S. & Mezger, K. Formation of Paleoarchean-Mesoarchean Na-rich (TTG) and K-rich granitoid crust of the Singhbhum craton, eastern India: constraints from major and trace element geochemistry and Sr-Nd-Hf isotope composition. *Precambrian Res.* **327**, 255–272 (2019).
38. Acharyya, S. K. Greenstones from Singhbhum craton, their Archaean character, oceanic crustal affinity and tectonics. *Proc. Natl Acad. Sci. India Sect. A* **63**, 211 (1993).
39. Jodder, J., Hofmann, A. & Ueckermann, H. 3.51 Ga old felsic volcanic rocks and carbonaceous cherts from the Gorumahisani Greenstone Belt – Insights into the Palaeoarchaean record of the Singhbhum Craton, India. *Precambrian Res.* **357**, 106109 (2021).
40. Bouvier, A., Vervoort, J. D. & Patchett, P. J. The Lu-Hf and Sm-Nd isotopic composition of CHUR: Constraints from unequilibrated chondrites and implications for the bulk composition of terrestrial planets. *Earth Planet. Sci. Lett.* **273**, 48–57 (2008).
41. Ranjan, S., Upadhyay, D., Pruseth, K. L. & Nanda, J. K. Detrital zircon evidence for change in geodynamic regime of continental crust formation 3.7–3.6 billion years ago. *Earth Planet. Sci. Lett.* **538**, 116206 (2020).
42. Chaudhuri, T., Wan, Y., Mazumder, R., Ma, M. & Liu, D. Evidence of enriched, Hadean mantle reservoir from 4.2-4.0 Ga zircon xenocrysts from Paleoarchean TTGs of the Singhbhum Craton, Eastern India. *Sci. Rep.* **8**, 7069 (2018).
43. Iizuka, T. et al. Reworking of Hadean crust in the Acasta gneisses, northwestern Canada: evidence from in-situ Lu–Hf isotope analysis of zircon. *Chem. Geol.* **259**, 230–239 (2009).
44. Roth, A. S. G. et al. Combined 147,146Sm-143,142Nd constraints on the longevity and residence time of early terrestrial crust. *Geochem. Geophys. Geosyst.* **15**, 2329–2345 (2014).
45. Bauer, A. M., Fisher, C. M., Vervoort, J. D. & Bowring, S. A. Coupled zircon Lu–Hf and U–Pb isotopic analyses of the oldest terrestrial crust, the >4.03 Ga Acasta Gneiss Complex. *Earth Planet. Sci. Lett.* **458**, 37–48 (2017).
46. Reimink, J. R. et al. Petrogenesis and tectonics of the Acasta Gneiss Complex derived from integrated petrology and 142Nd and 182W extinct nuclide-geochemistry. *Earth Planet. Sci. Lett.* **494**, 12–22 (2018).
47. Iizuka, T. et al. 4.2 Ga zircon xenocryst in an Acasta gneiss from northwestern Canada: Evidence for early continental crust. *Geology* **34**, 245–248 (2006).
48. Robin, C. M. I. & Bailey, R. C. Simultaneous generation of Archean crust and subcratonic roots by vertical tectonics. *Geology* **37**, 523–526 (2009).
49. van Hunen, J. & van den Berg, A. P. Plate tectonics on the early Earth: Limitations imposed by strength and buoyancy of subducted lithosphere. *Lithos* **103**, 217–235 (2008).
50. Turner, S., Rushmer, T., Reagan, M. & Moyen, J. F. Heading down early on? Start of subduction on earth. *Geology* **42**, 139–142 (2014).
51. Smithies, R. H. et al. Two distinct origins for Archean greenstone belts. *Earth Planet. Sci. Lett.* **487**, 106–116 (2018).
52. Tanaka, T. et al. JNdi-1: a neodymium isotopic reference in consistency with LaJolla neodymium. *Chem. Geol.* **168**, 279–281 (2000).
53. Roth, A. S. G., Scherer, E. E., Maden, C., Mezger, K. & Bourdon, B. Revisiting the 142Nd deficits in the 1.48 Ga Khariar alkaline rocks, India. *Chem. Geol.* **386**, 238–248 (2014).
54. Meissner, F., Schmidt-Ott, W.-D. & Ziegeler, L. Half-Life and alpha-ray energy of 146Sm. *Z. Phys. A Atom. Nuclei* **327**, 171 (1987).
55. Marks, N. E., Borg, L. E., Hutcheon, I. D., Jacobsen, B. & Clayton, R. N. Samarium-neodymium chronology and rubidium-strontium systematics of an Allende calcium-aluminum-rich inclusion with implications for 146Sm half-life. *Earth Planet. Sci. Lett.* **405**, 15–24 (2014).
56. Guitreau, M. et al. Hadean protocrust reworking at the origin of the Archean Napier Complex (Antarctica). *Geochem. Perspect. Lett.* **12**, 7–11 (2019).

Acknowledgements

This work was supported through the Swiss National Science Foundation (SNSF) grant #17452, Swiss Government Excellence Scholarship 2014.0848, SNSF Doc.Mobility fellowship P1BEP2_191759, and the Programme National de Planétologie (PNP) of CNRS/INSU, co-funded by CNES. Aimeryc Schumacher, Christiane Parmentier, Catherine Zimmerman, and Damien Cividini are thanked for their assistance during laboratory work. We thank Richard Carlson and two anonymous reviewers for constructive comments that helped to improve the quality of the manuscript.

Author contributions

A.M.: conception and design, sample collection, data acquisition/analysis and interpretation, wrote first original manuscript; G.C.: conception and design, data acquisition/analysis and interpretation, substantial revision of the manuscript; O.P.P.: sample collection, substantial revision of the manuscript; D.U.: sample collection, substantial revision of the manuscript; K.M.: conception and design, data interpretation; substantial revision of the manuscript.

Competing interests

The authors declare no competing interests.

Additional information

Supplementary information The online version contains supplementary material available at https://doi.org/10.1038/s43247-022-00341-9.

Correspondence and requests for materials should be addressed to Alessandro Maltese.

Peer review information *Communications Earth & Environment* thanks Richard Carlson and the other, anonymous, reviewers for their contribution to the peer review of this work. Primary Handling Editors: Joe Aslin, Heike Langenberg.

Reprints and permission information is available at http://www.nature.com/reprints

Publisher's note Springer Nature remains neutral with regard to jurisdictional claims in published maps and institutional affiliations.